Nucleation and Crystallization of Low-Crystallinity Polypropylene Followed in Situ by Hot Stage Atomic Force Microscopy

Holger Schönherr,[†,‡,§] Robert M. Waymouth,[*,‡,||] and Curtis W. Frank[*,†,‡]

Department of Chemical Engineering, Stanford University, Stanford, California 94305-5025, NSF MRSEC Center on Polymer Interfaces and Macromolecular Assemblies (CPIMA), Stanford University, Stanford, California 94305, and Department of Chemistry, Stanford University, Stanford, California 94305-5080

Received May 29, 2002

ABSTRACT: The isothermal crystallization of the ether-soluble fraction (ES) of elastomeric stereoblock polypropylene (ePP) was investigated in situ by hot stage atomic force microscopy (AFM) at temperatures between 30 and 60 °C. Owing to the low average tacticity of 21% ([*mmmm*]), this material possesses a very low degree of crystallinity (≤1% as determined by differential scanning calorimetry (DSC) and wide-angle X-ray scattering (WAXS)) in fully crystallized samples. Despite this low degree of crystallinity, hot stage AFM allowed us to study the nucleation and growth processes of crystallization in thin ES films in real time with nanometer resolution. The crystallization occurs in the form of lamellar crystals that develop from stable nuclei. Both metastable and stable primary nuclei have been visualized. Many crystals can be assigned to the α-phase of isotactic polypropylene (iPP) based on the observation of crosshatching. The lamellar growth rates are $<3 \times 10^{-3}$ μm/min and show a maximum between 40 °C and 45 °C. These results form the basis for a better understanding of the crystallization of ultralow crystallinity polypropylenes and likely other low crystallinity polymers.

Introduction

In recent years, polyolefin-based elastomers have attracted considerable interest due to their unique combination of facile synthesis, chemical inertness, and elastomeric properties.[1] Chief among these materials are copolymers of ethylene with alkenes, such as hexene or octene,[2,3] as well as elastomeric polypropylene (ePP) synthesized by, e.g., unbridged bis(2-arylindenyl) metallocene catalysts.[4−6] In general, all these thermoplastic elastomers[1,3,7] are characterized by a low degree of crystallinity.[1,8] The crystalline regions that are dispersed in the amorphous matrix have been postulated to provide physical cross-links for the amorphous elastomeric segments of the chain.[9] Hence, the mechanical properties of these materials are expected to be intimately related to the size and distribution of the crystalline regions in the amorphous matrix.

ePPs derived from unbridged bis(2-arylindenyl) metallocene catalysts and its fractions exhibit a low degree of crystallinity (1−40%)[8,10] but have been shown to crystallize in lamellar morphologies typical of much more highly crystalline polypropylenes.[13] Even the ether-soluble (ES) fraction of ePP with its degree of crystallinity of ≤1−2%, was found to crystallize with a lamellar habit.[8b,10] Such low degrees of crystallinity are at the resolution limit of X-ray scattering techniques such that in situ measurements of crystallization kinetics are practically impossible. Likewise, the traditionally applied techniques of DSC and polarized optical microscopy (POM) cannot be applied due to the lack of any clear signal. Owing to the important interdependence of crystallinity (and morphology) and mechanical properties, this and other low crystallinity materials clearly require new characterization techniques to thoroughly study the relevant material properties and to provide new insight into the crystallization behavior, i.e., crystallization kinetics and morphology development in real time.

Recent developments in the area of scanning probe microscopy promise in part to overcome these experimental limitations. Using hot stage atomic force microscopy, the groups of Vancso and Miles[11,12] carried out pioneering work leading to important new insights on the growth of lamellar crystals from the melt. Instead of growing with constant rate, as assumed in the prominent crystallization theories,[13] the lamellae grow with widely varying rates. A number of follow-up studies on various aspects of polymer crystallization have been published by various groups.[14−21]

In this paper, we focus on the extension of the hot stage AFM approach mentioned to the study of nucleation and growth processes in the ether-soluble fraction of elastomeric polypropylene. Our data clearly demonstrate the potential of AFM approaches at controlled temperatures in the study of the crystallization of low crystallinity polymers on the one hand, and provide novel insights into the hitherto unexplored crystallization behavior of a fraction of an important thermoplastic elastomer on the other hand.

Experimental Section

Materials and Sample Preparation. Elastomeric polypropylene (ePP) was synthesized by BP Amoco Chemical Company (PP-22010) in liquid propylene at 50 °C using bis(2-(3,5-di-*tert*-butylphenyl)indenyl)hafnium dichloride as catalyst.[22] Fractionation was carried out by successive solvent extraction of ePP with boiling diethyl ether under a nitrogen environment

* Corresponding authors. R.M.W.: telephone, 650 723-4515; fax, 650 725-0259; e-mail, waymouth@leland.stanford.edu. C.W.F.: telephone, 650 723-4573; fax, 650 723-9780; e-mail, curt@chemeng.stanford.edu.

† Department of Chemical Engineering, Stanford University.

‡ NSF MRSEC Center on Polymer Interfaces and Macromolecular Assemblies (CPIMA), Stanford University.

§ Present address: University of Twente, Faculty of Chemical Technology and MESA+ Research Institute, Department of Materials Science and Technology of Polymers, P.O. Box 217, 7500 AE Enschede, The Netherlands.

|| Department of Chemistry, Stanford University.

10.1021/ma0208335 CCC: $25.00 © 2003 American Chemical Society
Published on Web 03/11/2003

following the procedure reported previously.[8] As determined by high-temperature GPC, the ether-soluble (ES) fraction had a M_w of 147 kg/mol and a polydispersity M_w/M_n of 2.1. The fraction of isotactic dyads [*m*] in the polymer was 67%, while the fraction of isotactic pentads [*mmmm*] was 21% as determined by ^{13}C NMR. The samples investigated were initially melt pressed between two protective Teflon sheets (Mechanical Grade PTFE, McMaster-Carr) at 180 °C under a pressure of 500 psi in a hot press (model C, Carver, Menomonee Falls, WI). The final film thickness of 70 μm was achieved by manual pressing the films in the melt. After transfer of a small part of the film onto a small piece of a precleaned silicon wafer, the sample was placed on the AFM hot stage. All films were melted in situ on the hot stage in a gentle flow of preheated argon gas ($T \sim 80$ °C) at temperatures of >120 °C before being investigated at a preset isothermal crystallization temperature.[23]

Tapping Mode Atomic Force Microscopy (TM-AFM). The hot stage TM-AFM data were acquired in a home-built glovebox with a NanoScope III multimode AFM operated in tapping mode (Digital Instruments (DI), Santa Barbara, CA) using microfabricated silicon tips/cantilevers (Nanosensors, Wetzlar, Germany). To avoid possible degradation effects of the material, as well as contamination of the AFM cantilever by condensation of water or other contaminants that could affect the cantilever resonance frequency, the hot stage AFM experiments were carried out in a glovebox containing an argon gas atmosphere. The phase images shown here were subjected to a first-order plane-fitting procedure to compensate for sample tilt.[24] Amplitude and set point ratio were chosen such that the cantilever-tip assembly did not get trapped on the sample surface and that the imaging conditions warranted stiffness-dominated contrast in the phase images. Typical values for the rms amplitude were 3.0−6.0 V, while the set point amplitude ratio was adjusted to 0.5−0.6. The home-built hotstage, which is based on a Peltier element (MELCOR HOT2.0-18-F2A, Melcor, Trenton, NJ) connected to a home-built DC power supply, has been previously described.[20] Samples were attached to the Peltier using a minute amount of pressure-sensitive adhesive. The surface temperature of the Peltier element was monitored by a small thermocouple (IRCO-001 thermocouple J-type, diameter 0.001 in., Omega, Stamford, CT, connected to a Fluke 51 K/J thermometer, John Fluke Inc., Everett, WA), which was glued between the surface and a small piece of silicon wafer. The temperature reading of the thermocouple and the current applied to the Peltier were recalibrated by measuring the melting points of a series of *n*-alkanoic acids on silicon.[20] For the rather thick ES films studied, heat transfer from the sample through the gas phase to the cantilever-tip assembly leads to a surface temperature depression of >10 °C for (true) surface temperatures larger than 60 °C.[20] Since the film thickness (70 μm) and the thermal conductivities of polypropylene ($k_{PP} = 0.13$ W/(K m))[25] and argon ($k_{Ar} = 17.7 \times 10^{-3}$ W/(K m)),[26] are known, this effect can be accounted for assuming steady-state one-dimensional heat transfer (for details see ref 20).

Results

Following the complete melting of the polypropylene films on the AFM hot stage, the crystallization of lamellar crystals was imaged in situ under isothermal conditions by TM-AFM at temperatures between 30 and 60 °C. For all temperatures, the nucleation and growth of lamellar crystals was directly observed (Figure 1). Nucleation refers here to the appearance of ∼10−20 nm-sized stiff features in the previously homogeneous, featureless melt. These crystallites develop into individual and bundled rodlike features at the surface of the elastomer films, which slightly elevated in the height image (no data presented). As shown in Figure 1, TM-AFM phase images provide excellent contrast between the soft featureless melt and the stiff crystallites embedded in the melt at all temperatures.[27,28] Two different morphologies were observed: (1) a clear crosshatched morphology[29,30] and a flowerlike bundled morphology. While the crosshatched morphology was detected primarily at the early stage of the crystallization process, the flowerlike morphology often became prevalent at later stages. The angles between crosshatched lamellae of 80 ± 4° are independent of the crystallization temperature and were observed over the whole temperature range. On the basis of a large body of literature, these lamellae can be unequivocally assigned to the α-modification of iPP.[29,30]

The crystals appear as rodlike features with a typical width of ∼12−25 nm, depending on the radius of curvature of the particular AFM tip. This average (convoluted) thicknesses of the crystalline features was measured in cross-sectional plots. Owing to tip convolution, any quantitative determination of the thicknesses of these features from TM-AFM images leads to a considerable overestimate.[31]

While these crystallites are clearly observed by TM-AFM phase imaging, the overall crystallinity is *very* low. In the DSC scans and WAXS traces shown in Figure 2 for the same batch of ES, no more than 1 ± 1% crystallinity can be detected.[10] The quantitative analysis of the crystallization *kinetics* by traditional methods, such as DSC or WAXS, is thus a priori impossible. In contrast, hot stage AFM and the sensitive phase imaging technique allowed us to follow the crystallization of ES in real time. In Figures 3 and 4 different stages of lamellar development are depicted. These images are snapshots of a consecutively captured movie of typically several tens to hundreds of images. Since the lamellar growth rates (vide infra) are very small, the crystallization processes can be followed in unprecedented detail and with high relative temporal resolution.

Figure 3 shows two subsequently captured AFM images of very early stages of the crystallization at $T =$ 41 °C. Three main observations are noteworthy. First, we observe the disappearance of several bright spots (see squares labeled 1−3). Second, in the circle denoted A, a bright spot appears. Finally, one of the reference features grows in size (black circle B), while three faintly bright spots in the black ellipse do not change their appearance. The third reference point C is likely a dust particle. In subsequently captured images (data not shown), several of the small bright spots, including the three reference spots in the ellipse, start to grow into lamellae, and in a few cases, branching events can be observed.

The development of a number of crosshatched lamellae in the α-modification can be recognized in Figure 4. These images were acquired over a period of more than 20 h at 34 °C. At later stages, several bundled crystallites develop in the top left corner of the scanned area starting from a subsequently spontaneously nucleated crystal.[32]

In addition to early stages of crystallization in the quiescent melt, we were able to image the homoepitaxial nucleation of iPP daughter lamellae on dominant mother lamellae, a process that eventually leads to the crosshatched lamellar morphology shown in Figures 1 and 4. Individual nucleation or early growth events were resolved as the appearance of a (bright) blob of material shown in Figure 5. It is interesting to note that after the nucleation, the growth rates of the different daughter lamellae seen in Figure 5 differ significantly. While the lamellae labeled 1 and 3 grow steadily after nucle-

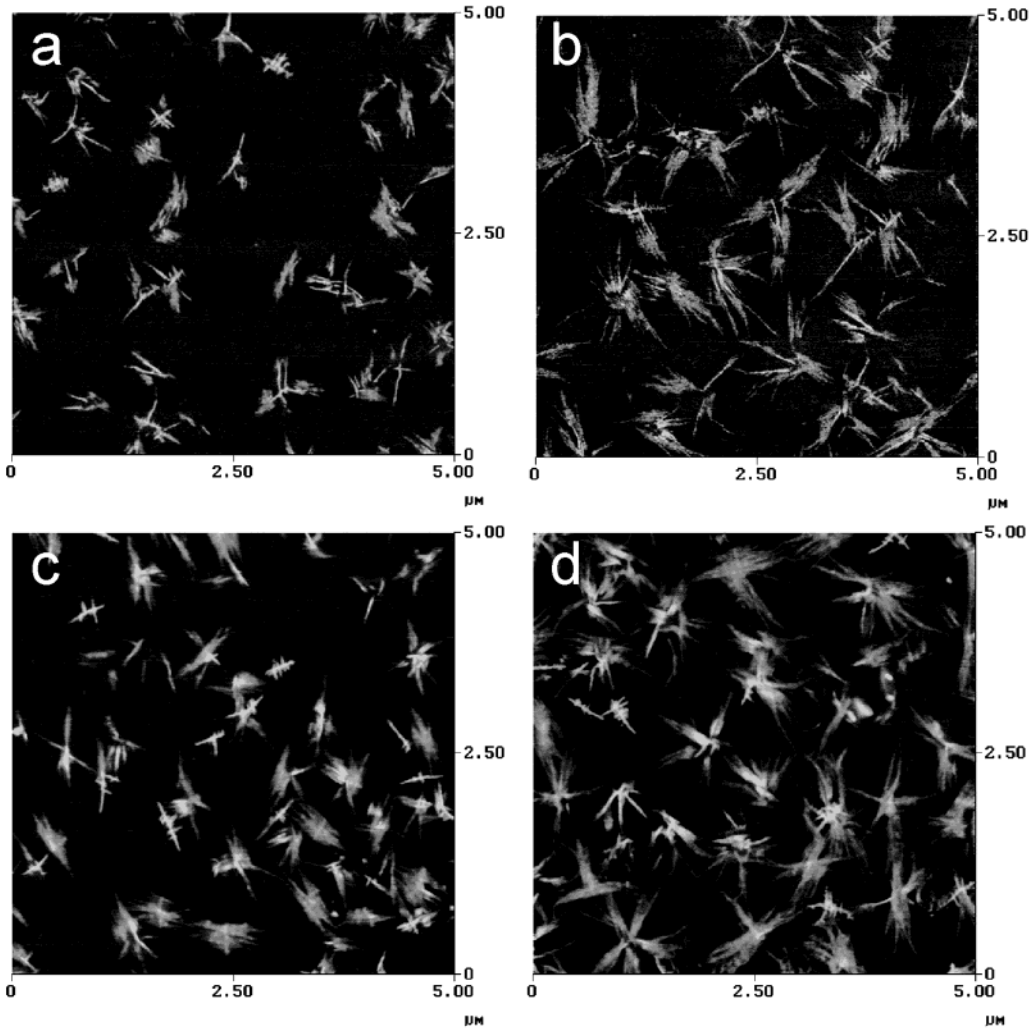

Figure 1. Hot stage TM-AFM micrographs (phase mode)[24] recorded in situ at 34 °C (a, early stage; b, late stage) and 54 °C (c, early stage; d, late stage). The matrix with dark phase contrast corresponds to the uncrystallized polymer melt, while the bright features are attributed to lamellar crystals. Different stages of crystallization including single lamellae in edge-on orientation, isolated crosshatched lamellae, and a bundled flowerlike morphology can be recognized. For a close-up view of crosshatched lamellae, see Figure 4.

ation, the lamellar patch labeled 2 remains dormant before growing with reduced rate compared to 1 and 3.

The initial growth rates of individual lamellae are linear in time, which is consistent with the polymer-typical nucleation and growth process (Figure 6).[13] At later stages of crystallization, the rates slow (no data shown), which can be attributed to the apparent lack of sufficiently long and perfect stereoregular sequences in the fraction investigated. From the analysis of the length of many individual lamellae grown isothermally at various temperatures, a growth rate−temperature plot was constructed (Figure 7). The curve shows a maximum at ca. 40−45 °C, and the highest growth rates are $<3 \times 10^{-3}$ μm/min.

Discussion

As shown here for the first time in polypropylene-based materials, the early and later stages of the isothermal crystallization of lamellae of iPP (in the ether-soluble fraction of elastomeric polypropylene) were studied by hot stage AFM. Despite the ultralow degree of crystallinity of ≤1% in fully crystallized samples, tapping mode phase imaging allowed us to follow the nucleation and crystallization of ES in situ. Considering the imaging conditions and, in particular, the amplitude damping used in the experiments, the contrast in tapping mode phase imaging is assumed to be based on differences in stiffness of the crystals and the melt.[27,33] While the TM-AFM phase images allow one to detect the polymer crystallites in the melt, these images provide no insight into the degree of perfection of the crystals. Hence, the absolute degree of crystallinity cannot be determined quantitatively from an estimation of the areas with different phase contrast.[34]

The observed elongated features (see Figures 1 and 4) can be assigned to edge-on oriented lamellae, as discussed in detail in a previous paper.[10] Taking the tip convolution effects into account, the average (convoluted) thicknesses of the lamellae of ∼12−25 nm compare favorably with lamellar thicknesses reported for iPP in the literature.[35,36] In particular, the observation of crosshatching for all temperatures investigated in this study and the polymer-typical linear growth rate corroborate this assignment.[37] The exclusive presence of edge-on oriented lamellae in the thin film samples investigated in this study is consistent with reports that lamellae in polyolefins, and PP in particular, grow preferentially in edge-on orientation in thin films.[38]

The origin of the two different types of micromorphology observed, i.e., crosshatching and bundled flowerlike

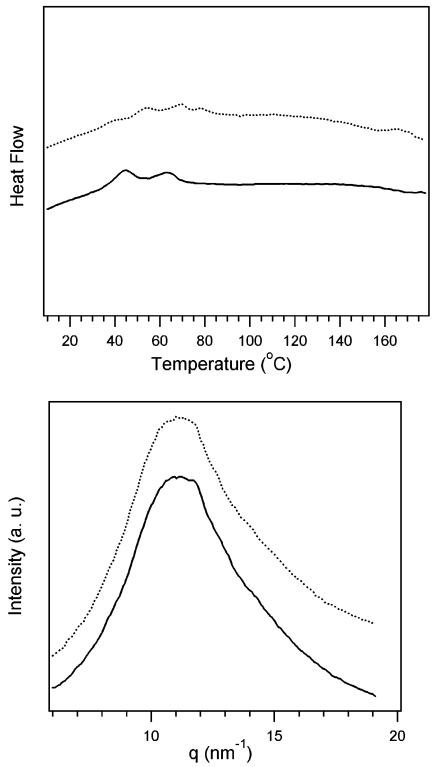

Figure 2. DSC endotherm scans (top) and WAXS profiles (bottom) of isothermally (solid lines) and nonisothermally (dotted lines) crystallized ES (adapted from ref 10).

morphology, cannot be unequivocally identified. One possibility is the presence of two different polymorphs (α and β). Alternatively, the coexistence of two qualitatively different morphologies, e.g., chain-folded lamellar and fringed micellar morphologies, or the absence of lamellar branching for a significant fraction of α-phase lamellae could explain the observations. While we have definite proof for the presence of the α-modification in the case of crosshatched lamellae, the other possibilities cannot be differentiated based on the available information. The analysis of the WAXS pattern (see Figure 2) remains inconclusive, since the intensities are too low to make a definite statement or resolve broad peaks of likely multiple polymorphs.

The magnitude of the growth rates determined by an analysis of the length of individual lamellae ($<3 \times 10^{-3}$ μm/min) is many orders of magnitude lower than for conventional semicrystalline polymers (Figures 6 and 7). A direct comparison of single lamellar growth rates is difficult due to lack of suitable literature data; however, isotactic polypropylenes are known to crystallize rapidly with half-crystallization times of several minutes to tens of seconds depending on undercooling.[39] Thus, one important effect of the polymer architecture, i.e., the stereoblock microstructure with its low isotacticity, seems to be a decrease of the magnitude of the growth rates. Owing to this microstructure of the ePP material and its fractions,[6,8,10] the enrichment of long defects and atactic sequences close to the interface between lamellae and melt seems plausible. Hence, it would be consistent to assume a reduced growth rate and a reduced fraction of available sites where lamellar growth by stem attachment, but also homoepitaxy, could occur on already-grown lamellar crystals. The observation of low growth rates on one hand and the observation of crosshatching at early stage of the crystallization

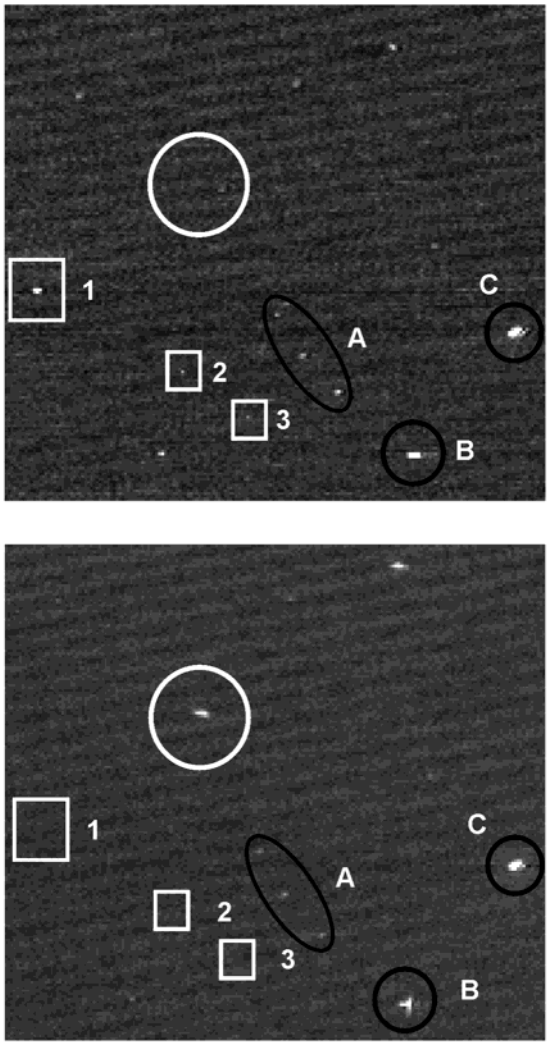

Figure 3. Early stages of ES crystallization followed by hot stage AFM at 41 °C (TM-AFM phase images).[24] The black circles indicate dormant nuclei (A), as well as growing lamellae (B) and a dust particle (C) as reference points. The white squares show the positions of three nuclei (1−3) that became unstable and disappeared, while the white circle shows the appearance of a nucleus from the previously homogeneous melt. The time elapsed between the two images were captured was 256 s (image size 3.3 μm × 3.0 μm).

and flowerlike overgrowth at later stages, on the other hand, are consistent with this interpretation.[40]

The appearance of lamellar crystals in the melt following the initial nucleation was visualized in several cases (see Figures 3 and 4). A high precision and high resolution imaging of this process is still limited by thermal drift during the stabilization period of the force microscope. This period sets in after the inevitable temperature drop from the melting temperature to the crystallization temperature and lasts for several minutes. This time is usually sufficient to detect nuclei in a large area scan (5−10 μm^2), but the pixel resolution of the commercial AFM used (512 × 512 pixels^2) limits the actual resolution in these cases. Hence, the shape and dimensions of the nuclei cannot be analyzed. However, as shown in Figure 3, this does not rule out the *detection* of these early aggregates.

In particular, we have observed the appearance *and* disappearance of very small features that possess a positive phase shift with respect to the melt (feature A vs features 1, 2, and 3 in Figure 4). Since a nucleus is

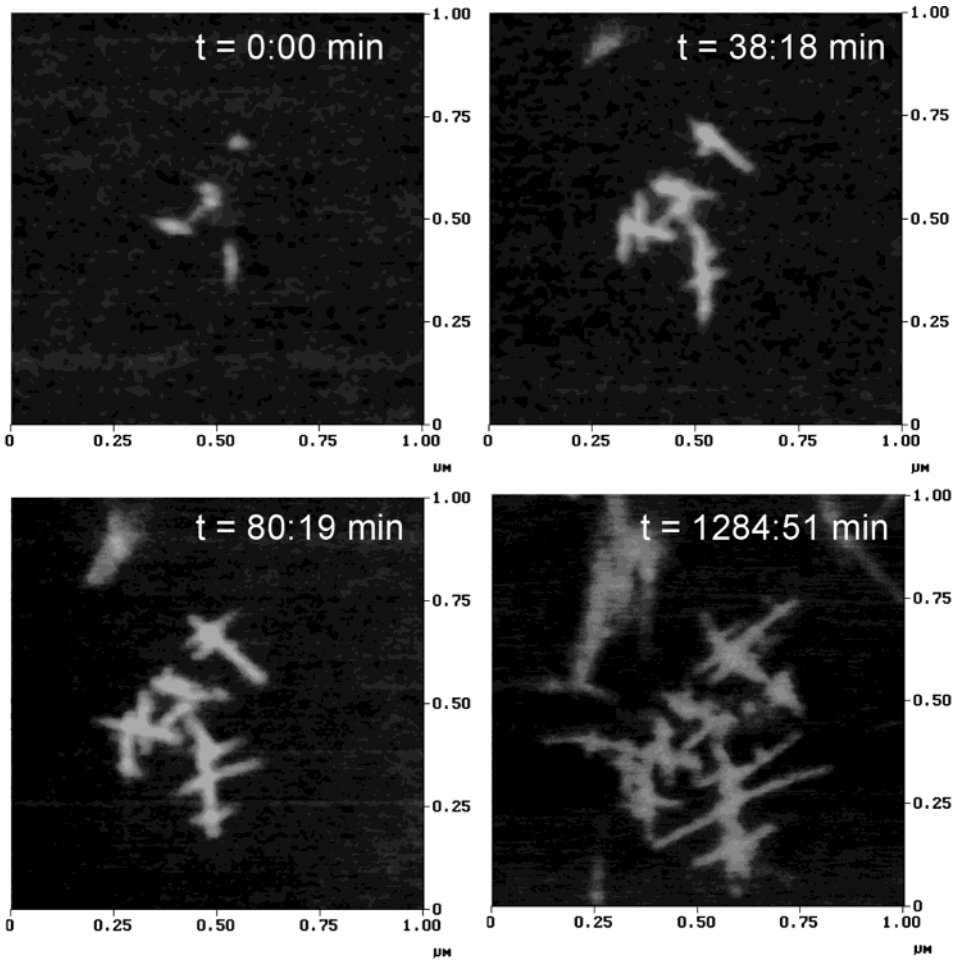

Figure 4. Various stages of α-phase lamellae (central area) in ES as unveiled by TM-AFM (phase mode)[24] at 34 °C.

assumed to be a single crystal-like entity,[41] this stiffness contrast is expected at any stage of its development. The features subsequently grow into lamellar crystals. Some of these lamellae show crosshatching and hence are composed of α-iPP. These observations are at least consistent with the view that polymer crystallization starts by the formation of (stable) nuclei. If a nucleus becomes stable, it can grow further to develop a lamellar habit (e.g., feature B in Figure 3), while it may also disintegrate in case it is unstable (e.g. features 1, 2, and 3).[42] The limited resolution in the experiment mentioned above makes the unequivocal differentiation of small growing crystallites and (meta)stable nuclei difficult, but the disappearance of stable growing crystals would be in conflict with the nucleation theory. Thus, our results suggest that indeed primary nuclei have been visualized.[42]

The resolution of the TM-AFM experiment on homoepitaxial nucleation (Figures 4 and 5) is higher compared to Figure 3 since the observed events take place after the AFM has stabilized. Hence, smaller scan sizes are feasible and the imaging conditions are stable. The development of crosshatching begins with the deposition of a patch of daughter lamella, which is detected due to its increased stiffness relative to the melt. This first patch may grow rapidly into the surrounding melt, or, as clearly seen in Figures 4 and 5, it may remain dormant for considerable time. This behavior is likely related to the lack of crystallizable material in the region near the growth front or the incorporation of an isotactic PP-rich segment of the chain, which is followed by a very long atactic block along the incorporated chain. If the isotactic PP-rich segment is not removed by detachment of the already attached segment, this may lead to the termination of the growth at this particular location.

Considering the literature[11−21,42] and this work, it becomes evident that detailed studies of very early stages of crystallization following the initial nucleation events, as well as lamellar growth at high undercoolings, of *commercially relevant* semicrystalline polymers, such as iPP, may be viewed currently as difficult or still impossible using hot stage AFM.[42] Such studies of materials with orders of magnitude faster crystallization rates than the ES described here may still require improvements of AFM instrumentation (scan rates) and similarly, improvements of the thermal stability of the AFM setups.[43] Recent developments in scanning probe microscopy hardware in this respect are very promising.[44] As we have shown here, hot stage AFM possesses a unique sensitivity to differences in stiffness *combined with* a high spatial resolution. These features make this approach highly attractive to possibly obtain in the future the necessary microscopic and nanoscopic information needed to develop better models and better understanding of nucleation and growth in polymer crystallization.

Conclusions

Using hot stage AFM, we have followed the isothermal crystallization of the ether-soluble (ES) fraction of elastomeric stereoblock polypropylene (ePP) in situ at

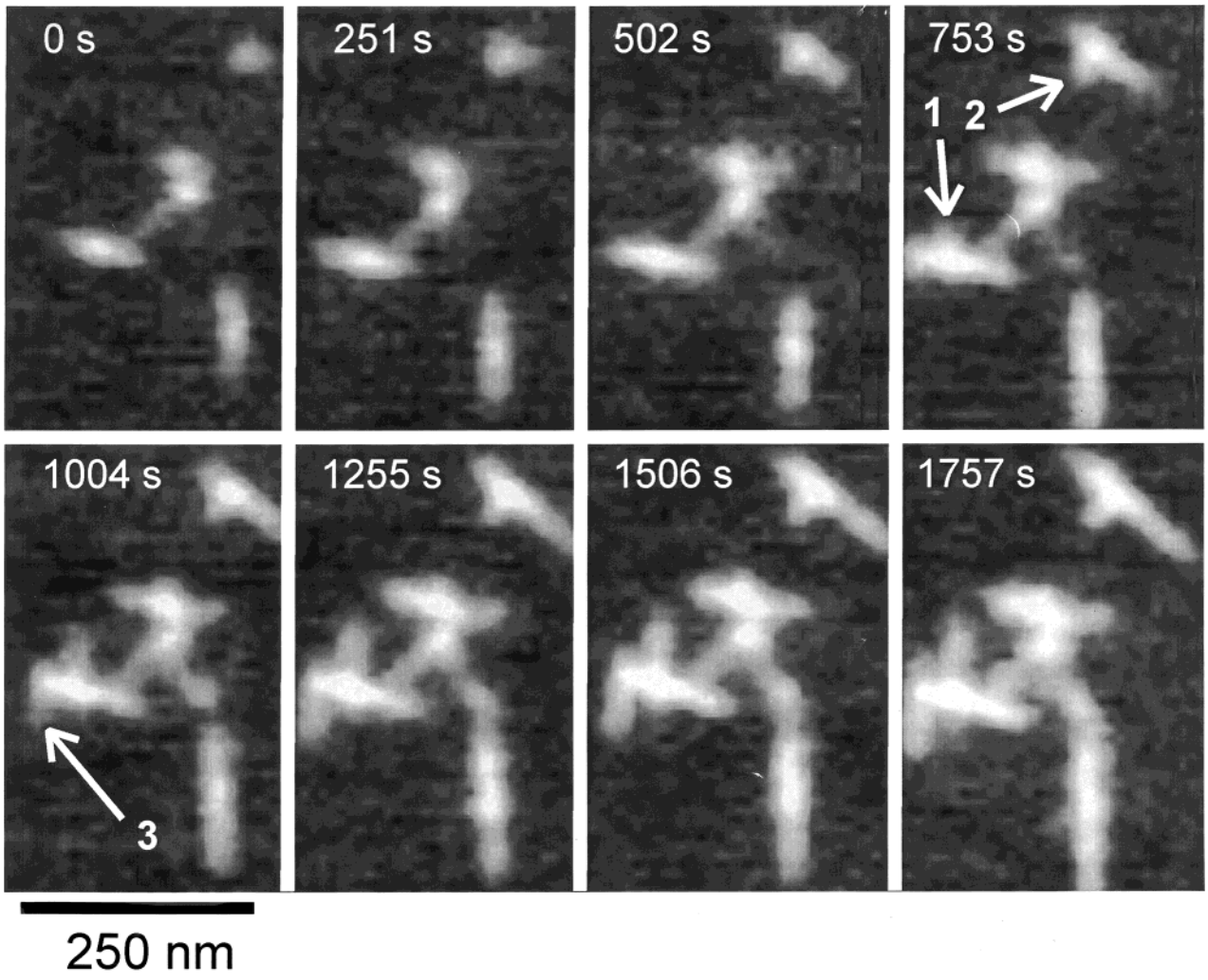

Figure 5. Growth of daughter lamellae nucleated on mother lamellae leads to a crosshatched morphology as imaged by TM-AFM at 34 °C (phase images).[24] The dark arrows point at homoepitaxial nucleation events; the subsequent growth of lamellar crystals proceeds with different rates. While lamellar patches *1* and *3* grow steadily, patch *2* remains dormant for at least 500 s before growing slowly. The pixel size is ∼ 2 nm.

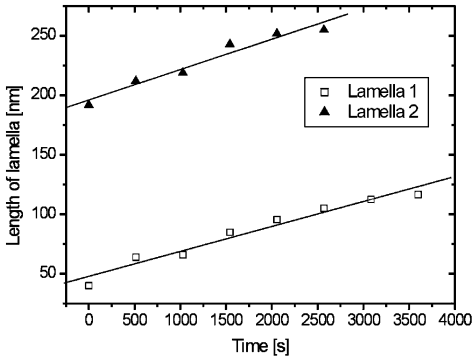

Figure 6. Initial lamellar growth rate of ES lamellae crystallized at 34 °C.

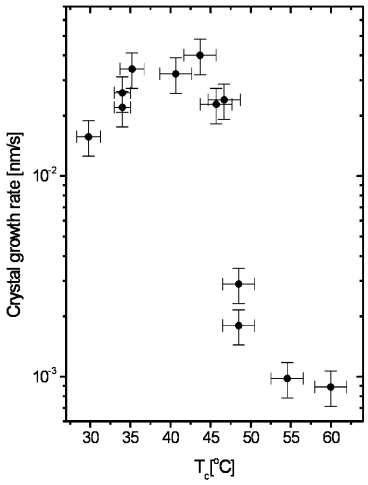

Figure 7. Logarithmic plot of initial lamellar growth rates vs isothermal crystallization temperature T_c.

temperatures between 30 and 60 °C. This high-resolution, real-space technique allowed us to study lamellar crystallization processes following the initial nucleation events in thin ES films with nanometer resolution. α-Phase polypropylene lamellae were identified based on the observation of crosshatching. The lamellar growth rates were measured quantitatively as a function of crystallization temperature. The fastest growth occurred at ca. 40−45 °C with a lamellar growth rate of $<3 \times 10^{-3}$ μm/min. These results constitute the first lamellar-level information on iPP crystallization studied in situ from the melt by AFM and form the basis for a better understanding of the crystallization of ultralow crystallinity polypropylenes and likely other low crystallinity polymers.

Acknowledgment. The authors acknowledge the contributions of Larry E. Bailey in the construction of

the hot stage and Willy Wiyatno in sample preparation and additional characterization. H.S. gratefully acknowledges financial support by the Deutsche Akademischer Austauschdienst (DAAD) in the framework of the "Hochschulsonderprogramm III" and the NSF MRSEC Center on Polymer Interfaces and Macromolecular Assemblies (CPIMA) under DMR 9808677.

References and Notes

(1) *Thermoplastic Elastomers*, 2nd ed.; Holden, G., Legge, N. R., Quirk, R. P., Schroeder, H. E., Eds.; 1996.
(2) Ho, T.; Martin, J. M. In *Metallocene-Based Polyolefins*; Scheirs, J., Kaminsky, W., Eds.; Wiley: Chichester, England, 2000; Vol. 2, pp 175−203.
(3) For a morphological investigation of polyethylene copolymers, see: Bensason, S.; Minick, J.; Moet, A.; Chum, S.; Hiltner, A.; Baer, E. *J. Polym. Sci., Part B: Polym. Phys.* **1996**, *34*, 1301.
(4) (a) Collette, J. W.; Tullock, C. W.; MacDonald, R. N.; Buck, W. H.; Su, A. C. L.; Harrel, J. R.; Mülhaupt, R.; Anderson, B. C. *Macromolecules* **1989**, *22*, 3851, 3858. (b) Ittel, S. D. *J. Macromol. Sci. Chem.* **1990**, *A27*, 9.
(5) (a) Mallin, D. T.; Rausch, M. D.; Lin, Y. G.; Dong, S.; Chien, J. C. W. *J. Am. Chem. Soc.* **1990**, *112*, 2030. (b) Bravakis, A. M.; Bailey, L. E.; Pigeon, M.; Collins, S. *Macromolecules* **1998**, *31*, 1000. (c) Dietrich, U.; Hackmann, M.; Rieger, B.; Klinga, M.; Leskelae, M. *J. Am. Chem. Soc.* **1999**, *121*, 4348. (d) Dreier, T.; Erker, G.; Frohlich, R.; Wibbeling, B. *Organometallics* **2000**, *19*, 4095.
(6) (a) Coates, G. W.; Waymouth, R. M. *Science* **1995**, *267*, 217. (b) Bruce, M. D.; Coates, G. W.; Hauptman, E.; Waymouth, R. M.; Ziller, J. W. *J. Am. Chem. Soc.* **1997**, *119*, 11174.
(7) Ho, T.; Martin, J. M. in *Metallocene-Based Polyolefins*; Scheirs, J., Kaminsky, W., Eds.; Wiley: Chichester, England, 2000; Vol. 2, p 175.
(8) (a) Carlson, E. D.; Krejchi, M. T.; Shah, C. D.; Terekawa, T.; Waymouth, R. M.; Fuller, G. G. *Macromolecules* **1998**, *31*, 5343. (b) Hu, Y.; Carlson, E. D.; Waymouth, R. M.; Fuller, G. G. *Macromolecules* **1999**, *32*, 3334. (c) Kravchenko, R.; Masood, A.; Waymouth, R. M.; Myers, C. L. *J. Am. Chem. Soc.* **1998**, *120*, 2039. (d) Carlson, E. D.; Fuller, G. G.; Waymouth, R. M. *Macromolecules* **1999**, *32*, 8094.
(9) Natta, G. *J. Polym. Sci.* **1959**, *34*, 531.
(10) Schönherr, H.; Wiyatno, W.; Pople, J.; Frank, C. W.; Fuller, G. G.; Gast, A. P.; Waymouth, R. M. *Macromolecules* **2002**, *35*, 2654.
(11) (a) Pearce, R.; Vancso, G. J. *Macromolecules* **1997**, *30*, 5843. (b) Pearce, R.; Vancso, G. J. *Polymer* **1998**, *39*, 1237.
(12) Schultz, J. M.; Miles, M. J. *J. Polym. Sci., Part B: Polym. Phys.* **1998**, *36*, 2311.
(13) For an overview see e.g.: (a) Wunderlich, B. *Macromolecular Physics*; Academic Press: New York, 1973, 1976, 1980; Vol. 1, Vol. 2, Vol. 3. (b) Bassett, D. C. *Principles of Polymer Morphology*; Cambridge University Press: Cambridge, England, 1981. (c) Strobl, G. *Polym. Phys.*; Springer: Heidelberg, Germany, 1997. (d) Gedde, U. *Polymer Physics*, 1st ed.; Kluwer: Academic Publishers: Dordrecht, The Netherlands, 1995.
(14) Studies on polymer crystallization close to room temperature (without active control of the specimen temperature) have been reported: (a) Hobbs, J. K.; McMaster, T. J.; Miles, M. J.; Barham, P. J. *Polymer* **1998**, *39*, 2437. (b) McMaster, T. J.; Hobbs, J. K.; Barham, P. J.; Miles, M. J. *Probe Microsc.* **1997**, *1*, 43. (c) Li, L.; Chan, C.-M.; Yeung, K. L.; Li, J.-X.; Ng, K.-M.; Lei, Y. *Macromolecules* **2001**, *34*, 316.
(15) Kikkawa, Y.; Inoue, Y.; Abe, H.; Iwata, T.; Doi, Y. *Polymer* **2001**, *42*, 2707.
(16) Basire, C.; Ivanov, D. A. *Phys. Rev. Lett.* **2000**, *85*, 5587.
(17) Zhou, W.; Cheng, S. Z. D.; Putthanarat, S.; Eby, R. K.; Lotz, B.; Magonov, S. N.; Hsieh, E. T.; Geerts, R. G.; Palackal, S. J.; Hawley, G. R.; Welch, M. B. *Macromolecules* **2000**, *33*, 6861.
(18) (a) Vancso, G. J.; Beekmans, L. G. M.; Pearce, R.; Trifonova, D.; Varga, J. *J. Macromol. Sci. Phys.* **1999**, *B 38*, 491. (b) Beekmans, L. G. M.; Vancso, G. J. *Polymer* **2000**, *41*, 8975.
(19) (a) Hobbs, J. K.; Miles, M. J. *Macromolecules* **2001**, *34*, 353. (b) Hobbs, J. K.; Humphris, A. D. L.; Miles, M. J. *Macromolecules* **2001**, *34*, 5508.
(20) Schönherr, H.; Bailey, L. E.; Frank, C. W. *Langmuir* **2002**, *18*, 490.
(21) (a) Schönherr, H.; Waymouth, R. M.; Hawker, C. J.; Frank, C. W. *Polym. Mater. Sci. Eng.* **2001**, *84*, 453. (b) Schönherr, H.; Frank, C. W. *Macromolecules* **2003**, *36*, 1188−1198, 1199−1208.
(22) Wiyatno, W.; Chen, Z.; Liu, Y.; Waymouth, R. M.; Brennan, K.; Krukonis, V. *Macromolecules*, submitted for publication.
(23) We have previously shown that lamellar crystals of ES melt at temperatures of <120 °C.[10]
(24) The TM-AFM phase images are presented without absolute color scale. Since the magnitude of the signals is affected by various scan parameters, such as precise amplitude of the free vibrating cantilever, and the setpoint amplitude ratio,[27,28] the values given by the AFM software can only be considered as relative values.
(25) Information from Matweb database (http://www.matweb.com).
(26) *Perry's Chemical Engineers' Handbook*, 6th ed.; Perry, R. H., Green, D., Eds.; McGraw-Hill: New York, 1984; pp 3−254.
(27) Magonov, S. N.; Elings, V.; Whangbo, M.-H. *Surf. Sci.* **1997**, *372*, L385.
(28) For a discussion of image contrast and its dependence on scanning conditions, see, e.g.: Bar, G.; Thomann, Y.; Brandsch, R.; Cantow, H.-J.; Whangbo, M.-H. *Langmuir* **1997**, *13*, 3807.
(29) Lotz, B.; Wittmann, J. C. *J. Polym. Sci., Polym. Phys.* **1986**, *24*, 1541 and references cited therein.
(30) (a) Bassett, D. C.; Olley, R. H. *Polymer* **1984**, *25*, 935. (b) Olley, R. H.; Bassett, D. C. *Polymer* **1989**, *30*, 399.
(31) Based on imaging of a calibration standard (Silicon grating GT01, Silicon MDT, Moscow, Russia), the radii of the tips used in our studies were estimated to be 5−15 nm.
(32) The imaging conditions were noninvasive as can be concluded from the absence of an increased or decreased rate of nucleation (and growth) in the scanned area compared to previously unscanned areas.
(33) If we approximate the modulus of the melt by the measured tensile modulus E_{ES} of the ES fraction (1.73 MPa: Wiyatno, W.; Pople, J.; Gast, A. P.; Waymouth, R. M.; Fuller, G. G. *Macromolecules* **2002**, *35*, 8488, 8498) and the modulus of the lamellae by E_{iPP} (1.0−1.7 GPa: *Polymer Handbook*, 4th ed.; Brandrup, J., Immergut, E. H., Eds.; Wiley: New York, 1989; pp V27), we can conclude a difference in modulus by 3 orders of magnitude. This difference is responsible for the pronounced contrast observed in the TM-AFM phase images.
(34) In addition, tip convolution effects and the penetration of the AFM tip into the melt, which results in a sampling of a surface-near volume, lead to a significant overestimation of the surface area occupied by crystallites.
(35) Lamellar thicknesses of 13−17 nm were reported for crystallization temperatures of 120 and 130 °C, see: (a) Ceres, B. V.; Schultz, J. M. *J. Appl. Polym. Sci.* **1984**, *29*, 4183. Further comparable data can be found in: (b) Mezghani, K.; Campbell, R. A.; Philips, P. J. *Macromolecules* **1994**, *27*, 997.
(36) We did not carry out a quantitative deconvolution of the AFM images since it is not a priori clear whether and to what extent these lamellar features protrude from the surface and since the information/penetration depths[27] in our experiments are difficult to quantify.
(37) In addition, the melting point of these lamellar features of ca. 100−120 °C, as determined by hot stage AFM, is consistent with a lamellar morphology rather than a simple fringed micellar morphology. The stepwise increase in temperature in increments of 5 °C and the subsequent stabilization period of several minutes resulted in an approximate mean heating rate of 0.6 °C/min.[10]
(38) Bartczak, Z.; Argon, A. S.; Cohen, R. E.; Kowalewski, T. *Polymer* **1999**, *40*, 2367 and references cited therein.
(39) See for instance: Lamberti, G.; Titomanilo, G. *Polym. Bull. (Berlin)* **2001**, *46*, 231.
(40) Alternatively, the latter observation may indicate a transition from nucleation and growth to diffusion-controlled crystallization at later stages. A similar dendritic habit of crystals is well-known for a wide variety of materials.
(41) Geil, P. H. *Polymer Single Crystals*; Wiley-Interscience: New York, 1963.
(42) In a very recent paper, Lei et al. report on a similar observation of nuclei and embryonic crystals in poly(bisphenol A octane ether) observed by in situ AFM at room temperature (Lei, Y.-G.; Chan, C.-M.; Li, J.-X.; Ng, K.-M.; Wang, Y.; Jiang, Y.; Li, L. *Macromolecules* **2002**, *35*, 6751.).
(43) Ivanov, D. A.; Amalou, Z.; Magonov, S. N. *Macromolecules* **2001**, *34*, 8944.
(44) Sulchek, T.; Hsieh, R.; Adams, J. D.; Minne, S. C.; Quate, C. F.; Adderton, D. M. *Rev. Sci. Instrum.* **2000**, *71*, 2097.

MA0208335